LA-UR-16-28776
Approved for public release; distribution is unlimited.

Title: Assess How Changes in Fuel Cycle Operation Impact Safeguards

Author(s): Tobin, Stephen Joseph
Adigun, Babatunde John
Fugate, Michael Lynn
Trellue, Holly Renee
Sprinkle, James K.

Intended for: Report

Issued: 2016-11-14

Assess How Changes in Fuel Cycle Operation Impact Safeguards

Prepared for:
Office of Dismantlement and Transparency (NA-241) Concepts and Approaches
U.S. Department of Energy

Prepared by
S.J. Tobin, B.J. Adigun, M.L. Fugate, H.T. Trellue, and J.K. Sprinkle
Nuclear Engineering and Nonproliferation Division, NEN-5 Group

Los Alamos National Laboratory
Los Alamos, NM 87545 USA

October 2016

Contents

1 Introduction

In this report two research topics of interest to Concepts and Approaches are investigated. The motivation of joining them into one project is that both require (1) the simulation of fuel irradiation in a reactor and (2) the transport of gamma and neutron irradiation from the fuel to safeguards detectors. In the next two subsections the merits of each of the two safeguards applications are further introduced.

1.1 Can safeguards benefit from modern irradiation practices?

Since the beginning of commercial nuclear power generation in the 1960s, the ability of researchers to understand and control the isotopic content of spent fuel has improved. Here we list a few of the most significant improvements:

1. All aspects of simulation capability have improved immensely, from hardware (memory, clock speed, storage space) to computer code capability.
2. The nuclear data of a large range of relevant isotopes, including a wide variety of reaction cross-sections, has improved in accuracy.
3. Reactor operators have improved the instrumentation monitoring reactor core performance; hence, they understand better how the flux varies in different parts of the reactor at different times.
4. Following decades of experience, the research community is better prepared to simulate spent fuel irradiation.

Given the cumulative impact of the enhancements listed above, it is not surprising that both fuel assembly design and fuel assembly irradiation optimization have improved over the past 50+ years. The purpose of the research summarized in this sub-section is to investigate what, if any, consequence this evolution in reactor operation might have for nuclear safeguards. It is anticipated that the burnup and isotopics of the spent fuel should exhibit less variation over the decades as reactor operators irradiate each assembly to the optimum amount. In contrast, older spent fuel is anticipated to vary more in burnup and resulting isotopics for a given initial enrichment. Continuing with this thesis, modern fuel should be more uniform in composition, and thus, measured safeguards results should be easier to interpret than results from older spent fuel.

With spent fuel ponds filling up, interim and long-term storage of spent fuel will need to be addressed. Additionally after long periods of storage, spent fuel is no longer self-protecting and as such the IAEA will categorize it as more attractive; in approximately 20 years many of the assemblies from early commercial cores will no longer be considered self-protecting. This study will assess how more recent changes in the reactor operation could impact the interpretation of safeguards measurements.

1.2 Is there merit to measuring spent fuel attributes from cradle-to-grave?

The status quo for spent fuel assay in the safeguards context is that the overwhelming majority of spent fuel assemblies are not measured in a quantitative way except for those assemblies about to be loaded into a *difficult or impossible to access location* (dry storage or, in the future, a repository). The primary measurement approach used by the IAEA is qualitative rather than quantitative. The IAEA primarily measured the Cerenkov emission from the water around the fuel pins, while the

assemblies are packed into a rack at the bottom of a spent fuel pool, to verify that a given assembly is whole. In other words, when the assembly is still accessible to a state actor, or an insider, when it is cooling in a pool, the inspectorate does not have a measurement database that could assist them in re-verifying the integrity of that assembly. If, for example, the continuity-of-knowledge (COK) were lost; the inspectorates would be in the position of recovering from that lost COK, from a measurement perspective, **based only upon** what they measure after the loss of COK. It is the goal of this sub-section to make the case that the spent fuel safeguards regime would be strengthened if spent fuel assemblies were measured from discharge to loading into a *difficult or impossible to access location*. The primary driver for suggesting this shift in approach is the change in robotic technology and information technology in general. It should be possible, with minimal impact to the facility, to measure each assembly every time that it is moved in the pool with the first measurements being made at discharge. To give a mental image of the robot envisioned, consider a cylinder rolling up the side of the assembly as the assembly is lowered into the spent fuel rack. The cylinder would measure the neutron and/or gamma emission of the assembly; similar to a Fork Detector, the key difference is that, unlike with a Fork detector, measurements would be tracked and compared in time.

1.3 Physics background to the quantitative tracking of spent fuel attributes concept

After the fuel leaves the reactor, the isotopic content of the fuel still changes; yet, this variation is relatively simple and predictable as compared to what takes place during irradiation. This is due to the fundamental fact that when the fuel leaves the reactor the driver of the isotopic evolution in the fuel, the neutron flux, drops by roughly a factor of a billion from the reactor to the cooling pond. As a result the temporal change in the fuel after discharge is almost completely driven by radioactive decay with well known half-lives.

The concept being investigated assumes an initial 'baseline' measurement of an assembly, such as passive neutron and passive gamma, can be used for monitoring a given fuel assembly throughout the life of that assembly before it goes to a *difficult or impossible to access* location. We have decided to put this present research in the context of currently deployed instruments; hence, the question we will answer is how much more useful two Fork measurements of the same assembly separated in time would be to an inspectorate? The count rates measured later in time would need be consistent with the decay of key isotopes; if a smaller than anticipated result is obtained or the neutron and gamma signals do not both vary in the expected way with time, it could indicate that the item was tampered with (i.e., pins may be missing).

2 Research Approach

2.1 Irradiated fuel details

The expected detector response to a range of spent fuel assemblies was simulated with MCNP in order to gain insight into the practicality of both of the outlined technical tasks. From a simulation perspective, this can be thought of as a three-step process. First, 17x17 PWR assemblies, with a specified initial enrichment, are irradiated given a particular reactor operating history. Second, the isotopic mix is cooled for a selected cooling time. And finally the gammas and neutrons produced by the isotopes present are transported to the selected detectors of interest.

In the case of this research, the following initial enrichment and burnup combinations were selected.

1. 2 wt.%, 15 and 30 GWd/tU
2. 3 wt.%, 15 and 30 GWd/tU
3. 4 wt.%, 15, 30 and 45 GWd/tU
4. 5 wt.%, 15, 30, 45 and 60 GWd/tU

Each of these 11 assemblies were cooled for the following duration following their final discharge: 4 days, 14 days, 0.5 years, 1 year, 2 years, 3.5 years, 5 years, 10 years, 20 years, 30 years, 40 years and 80 years. Hence, there were a total of 132 assemblies.

With the intent of restricting ourselves to assemblies that typically exist within the normal operation of commercial fuel, the degree to which an assembly was irradiated was limited by its initial enrichment. As an example we did not irradiate a 2 wt.% assembly to 45 GWd/tU. Yet, it is an important point to note that several of these assemblies with relatively low burnups compared to initial enrichments are rarely available for measurements by the inspectorate as they still contain significant potential nuclear energy and will typically be irradiated additional cycles before being discharged from the core.

To reduce the cost of performing this scoping research, we leveraged past research performed as part of the NGSI-SF Project [1, 2]. The research interests of the NGSI-SF project were subtly different than our current goals; the NGSI-SF Project was interested in creating realistic assemblies with an isotopic diversity that could exist for the purpose of seeing how different NDA instruments would be sensitive to the various isotopic changes. In contrast, our interest is to access if each of our two concepts is a plausible safeguards approach. For this purpose we need assemblies like those in the real world, which were methodically irradiated under the constraints experience by a commercial reactor operator to optimally extract the nuclear potential energy embodied in them by virtue of their initial enrichment.

2.2 Detector setup

The final step in the simulation process is to transport neutrons and photons from the fuel assembly to detectors. In selecting detector material, a strong emphasis was placed on commercial off-the-shelf hardware, which is thought to be suitable for measurements located near spent fuel. The response of the following three detector materials were simulated for all 132 assemblies: fission chambers, ion chambers and a lanthanum bromide detector ($LaBr_3$). For a few assemblies, the response of a high purity germanium (HPGe) detector was also simulated.

For each of these 132 assemblies, two sets of simulations were performed, one for which neutrons were transported from the spent fuel to a detector, the fission chamber case, and one for which gamma-rays were transported: the ion chamber, $LaBr_3$ and HPGe cases. In Figure 1, the setup used for the fission chambers and ion chambers simulations is illustrated. The left side of the figure depicts a horizontal cross-section of the fuel and detector that cuts through a detector tube; the right side is a vertical cross-section in which the presence of two tubes on each side of the assembly is illustrated. Beneath the vertical and horizontal illustration is a magnified axial view of the fission and ion chambers. For the ion chamber case a tube with the following parameters was inserted in the polyethylene rectangles illustrated: 10 atm of N_2 gas, 2.5 cm diameter tube, active length of 15.5 cm. For the fission chamber case a tube with the following parameters was used: a total of 2.96 grams of 93 wt.% uranium in 2 fission chamber tubes, and an active length of 15.5 cm.

In Figure 2 the setup used for the simulated $LaBr_3$ and HPGe cases is illustrated; in both cases the crystal was cylindrical with a diameter of 5.08 cm and a height of 5 cm. The full width at half maximum (FWHM) of observed energy broadening in a physical detector is given by:

$FWHM = a + b\sqrt{E + cE}$. The Gaussian energy broadening parameters *a, b, and c* for the $LaBr_3$ detector setup were -0.005219, 0.046942, and -0.410624, respectively. In the HPGe detector setup, the Gaussian energy broadening parameters used were -0.00122206, 0.00341921, and -0.218813, respectively.

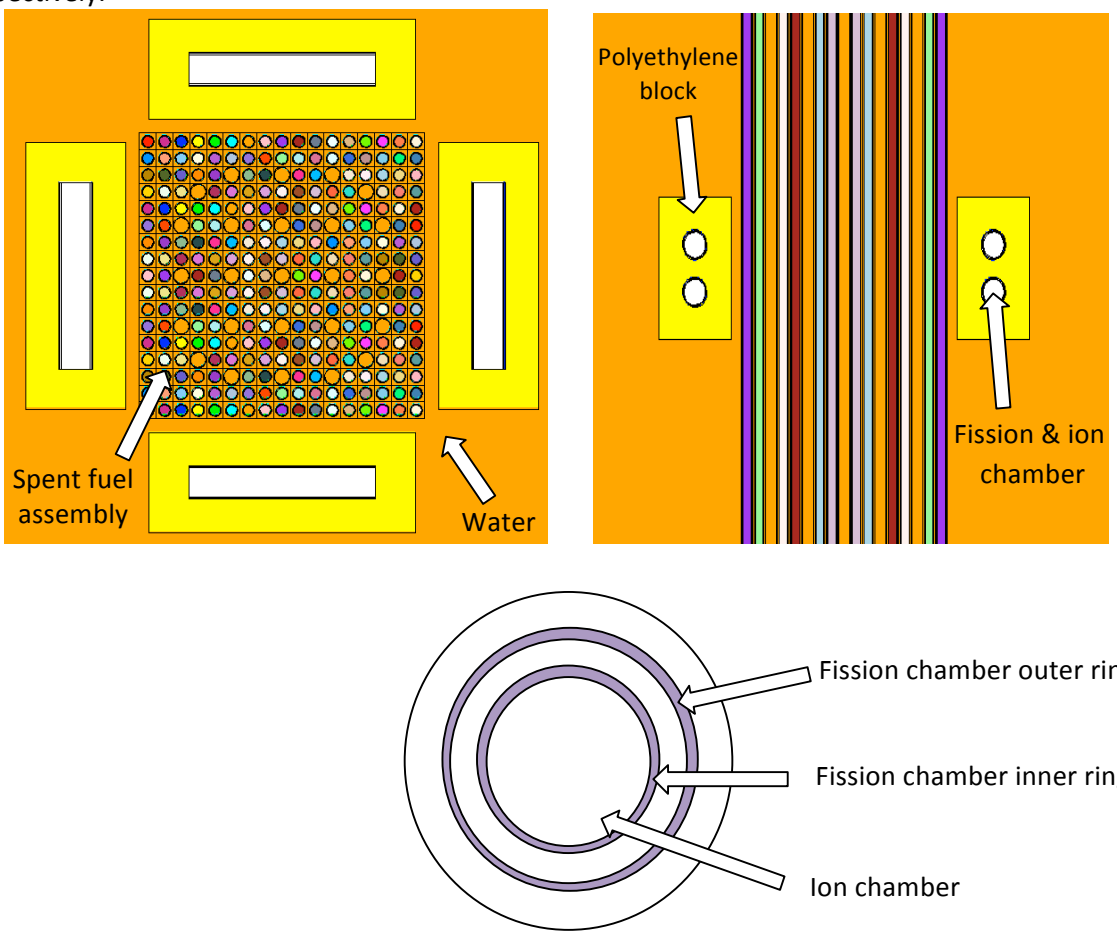

Figure 1. Depicted on the top left side is the horizontal cross-section of the fuel and detector; the cross-sectional cut goes through a detector tube on each side of the fuel. Depicted on the top right side is a vertical cross-section in which the presence of two tubes on each side of the assembly is illustrated. The bottom center figure depicts a not-to-scale illustration of the fission and ion chamber geometry.

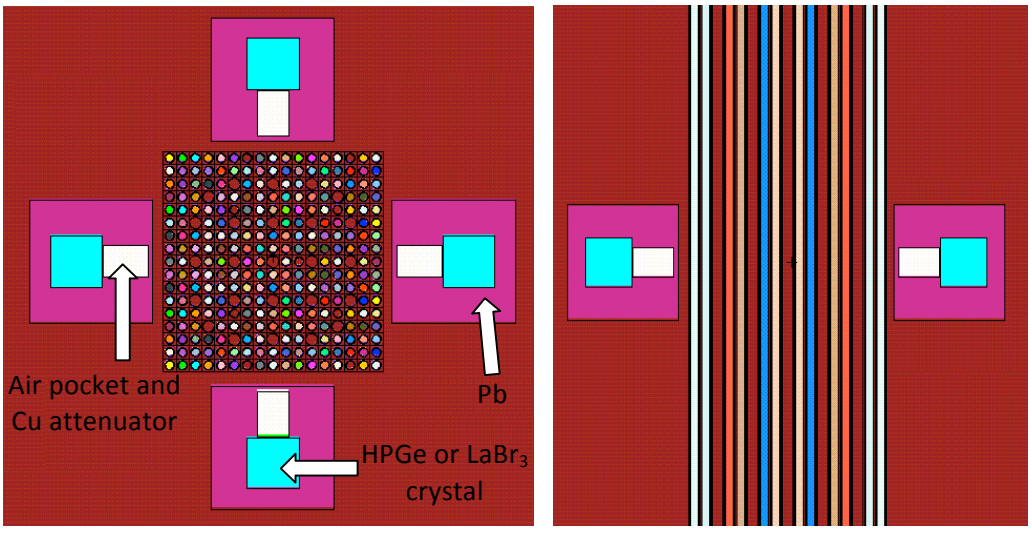

Figure 2. Depicted on the left side is the horizontal cross-section of the fuel and detector crystal material; on the right side is a vertical cross-section of the fuel and detector crystal material.

3 Simulated Results and Discussion

The utility of tracking the measured signature from a spent fuel assembly from cradle-to-grave is tightly coupled to how well the signature can be predicted at some future date. The conceptual application is that the inspectors, measuring a given assembly cooling in the pool, would know before they make a measurement that assembly A should have a predefined neutron count rate in the fission chambers and a current in the ion chambers based on past measurements and appropriate predictive algorithms. If the actual measurement deviated significantly from the predicted values, then a flag would be raised. As such, central to the current research is formulating predictive algorithms. In this section both the simulated "raw data" and the algorithms are presented.

3.1 Fission Chambers results and discussion

In the case of passive neutron production in an assembly, there are three primary production mechanisms: spontaneous fission, (α, n), and induced fission. The first two source terms increase rapidly with the irradiation of the spent fuel assembly while the fissionable material and thus the third term decreases relatively slowly.

Given that the dominant neutron production mechanism in most commercial spent fuel assemblies is the spontaneous fission of ^{242}Cm and ^{244}Cm with half-lives of 0.45 and 18.1 years [3, 4] respectively, the following algorithm was suggested:

$$Total\ Neutron\ Count\ Rate = A + Be^{-\lambda_b t} + Ce^{-\lambda_c t} \quad (1)$$

A, B and C which are functions of initial enrichment and burnup are constants, λ_b and λ_c are the decay constants for ^{242}Cm and ^{244}Cm, and t is time following discharge. In Figure 3, the simulated count rate is graphed vs. the predicted count rate for 4 different initial enrichment values. The predictive algorithm used in Figure 3 was formed using all the data points as input.

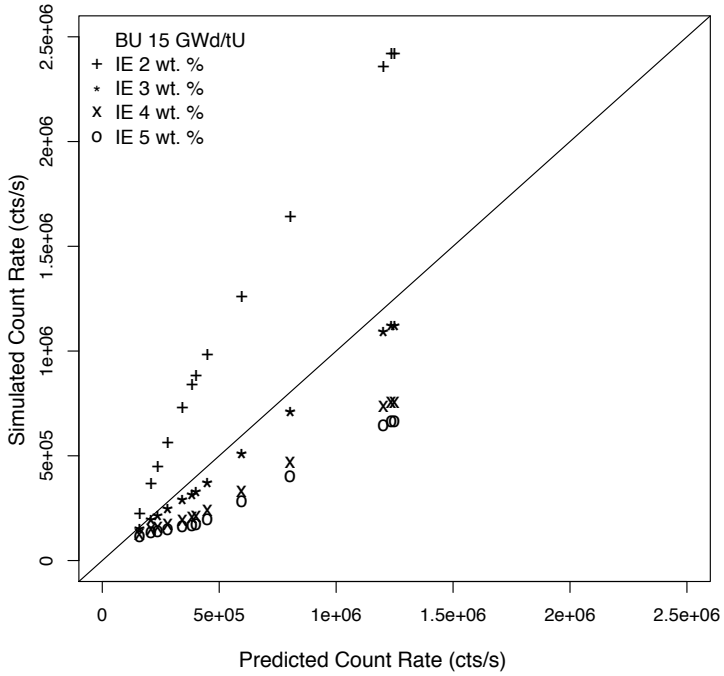

Figure 3. The simulated neutron count rate for the 8 fission chambers illustrated in Figure 1 is depicted as a function of the predicted count rate for all assemblies irradiated to 15 GWd/tU.

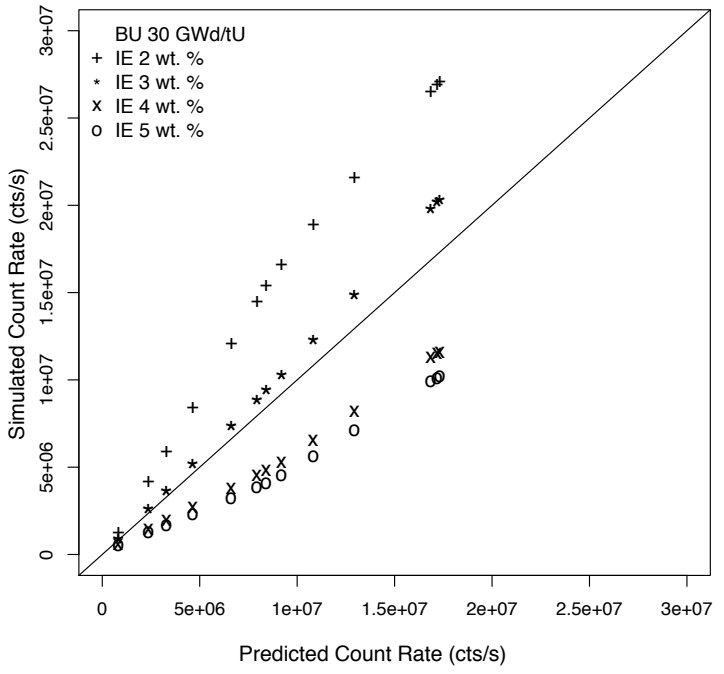

Figure 4. The simulated neutron count rate for the 8 fission chambers illustrated in Figure 1 is depicted as a function of the predicted count rate for all assemblies irradiated to 30 GWd/tU.

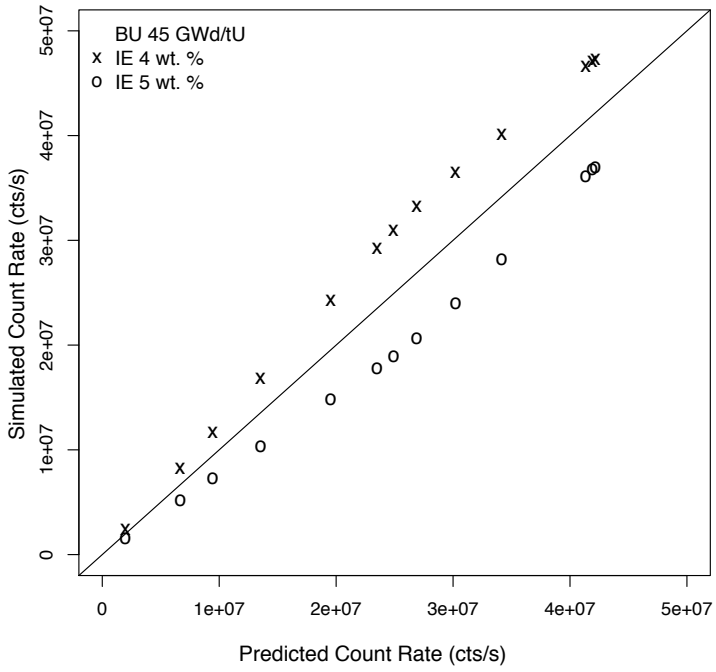

Figure 5. The simulated neutron count rate for the 8 fission chambers illustrated in Figure 1 is depicted as a function of the predicted count rate for all assemblies irradiated to 45 GWd/tU.

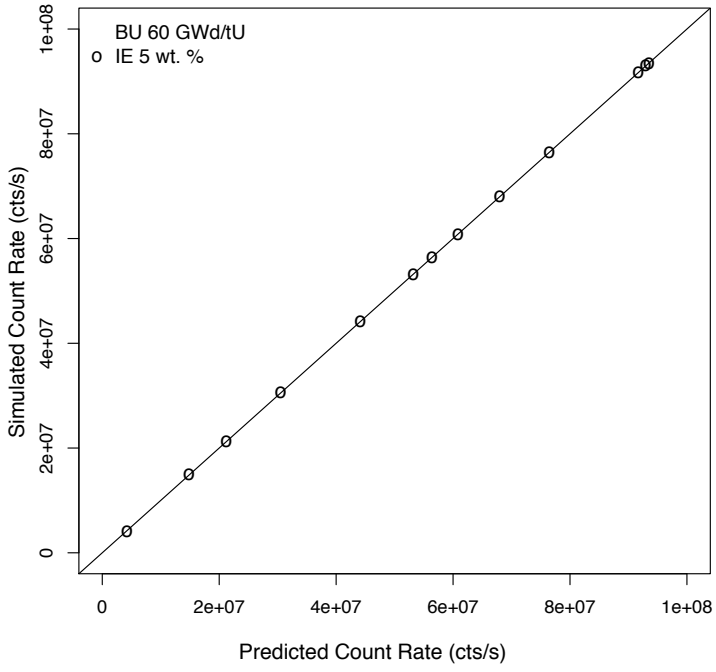

Figure 6. The simulated neutron count rate for the 8 fission chambers illustrated in Figure 1 is depicted as a function of the predicted count rate for all assemblies irradiated to 60 GWd/tU.

The following conclusions are made from Figures 3 to 6:

1. If burnup and initial enrichment are known, then the prediction of the total neutron count rate as a function of time after discharge is very well known. Because Figure 6 illustrates one initial enrichment and burnup case in isolation, the excellence of the fit is well demonstrated. Using Equation 1, with each individual initial enrichment and burnup case analysed separately for all the data illustrated in Figures 3 to 6, produced a standard deviation value of ~2% for all 11 cases [5]. Note that the estimated burnup of individual assemblies given by reactor operators are expected to be accurate to a 2% to 5% one standard deviation variation [6].

2. For a given burnup values, the initial enrichment has a strong impact, a factor of ~2.5, on the total neutron count rate as evident in Figures 3 and 4 for which 4 initial enrichment values were simulated. How to interpret this fact in the safeguards context is a point of extended discussion later in this report.

3. By comparing among Figures 3 to 6, the commonly stated empirical 3rd or 4th power scaling of the total neutron count rate with burnup is evident [7]. This is demonstrated in the fact that for the 5 wt.% assemblies, as burnup increases from 15, 30, 45, 60 GWd/tU, the total neutron count rate at discharge increased respectively from 0.7, 10.1, 36.8, 93.0 million counts/s.

3.2 Ion Chamber results and discussion

For gamma production in an assembly, as compared to neutron production, the situation is more complex, particularly in the first few years after discharge. From analyzing the data, a cooling time of 3.5 years proved to be a convenient dividing point. For spectra obtained at 3.5 years and after, a relatively simple trend line, similar in form to that used for neutrons, was created. Before 3.5 years, a more complex equation inclusive of short-lived and dominant gamma emitting isotopes contributing to the ion chamber current was used.

3.2.1 Cooling time from discharge to before 3.5 years

The gamma emission from an assembly before 3.5 years is dominated by numerous isotopes. During irradiation for the particular shuffling scheme examined, isotope production typically scaled either to flux or burnup; in certain cases, isotope production scaled to neither flux nor burnup. Upon discharge, these isotopes produced during irradiation that scaled to neither flux nor burnup constituted a huge portion of the gamma emitters [8]. These isotopes are typically short-lived with half-lives on the order of seconds, days, weeks or months [7]. Due to this, their effect on the gamma emission from an assembly cooling times less than 3.5 years is pronounced.

Initially, ten isotopes – ^{137}Cs, ^{95}Zr, ^{95}Nb, ^{144}Ce, ^{140}La, ^{134}Cs, ^{154}Eu, ^{103}Ru, ^{239}Np, ^{106}Rh – were selected for inclusion in Equation (2) to account for these short-lived high intensity gamma emitters. These ten isotopes selected accounted for ~98% of the gamma emissions from the assemblies at cooling times less than 3.5 years. However, after an iterative effort geared at reducing Equation (2) to the smallest number of terms possible while still attaining a high rate of predictability for the ion chamber current, four of these isotopes – ^{154}Eu, ^{103}Ru, ^{239}Np, ^{106}Rh – were dropped. As such, the prediction by Equation (2) omits several isotopes contributing to the ion chamber gamma current. In the worst case, the isotopes listed in Equation (2) accounted for only ~50% of the gamma emissions from a particular spent fuel assembly. The final algorithm suggested for predicting the ion chamber current is shown below, and its predictive capability is illustrated in Figure 7.

$$Ion\ Chamber\ Current = A + Be^{-\lambda_b t} + Ce^{-\lambda_c t} +$$

$$De^{-\lambda_d t} + Ee^{-\lambda_e t} + Fe^{-\lambda_f t} + Ge^{-\lambda_g t} \quad (2)$$

A, B, C, D, E, F and G, which are functions of initial enrichment and burnup, are constants, while λ_b, λ_c, λ_d, λ_e, λ_f and λ_g are the decay constant of ^{137}Cs, ^{95}Zr, ^{95}Nb, ^{144}Ce, ^{140}La, and ^{134}Cs, and t is time following discharge.

The following observations are made from Figure 7 and the exercise of predicting the ion chamber current at cooling times less than 3.5 years:

1. Equation (2), the terms in which have the temporal variation representative of 6 isotopes, provides an accurate prediction of the expected ion chamber current at all cooling times for all simulated assemblies with very little scatter.

2. For reasons of representing the physical reality, it is proposed that Equation (2) be revised to include the omitted terms for isotopes contributing to the gamma source term emissions.

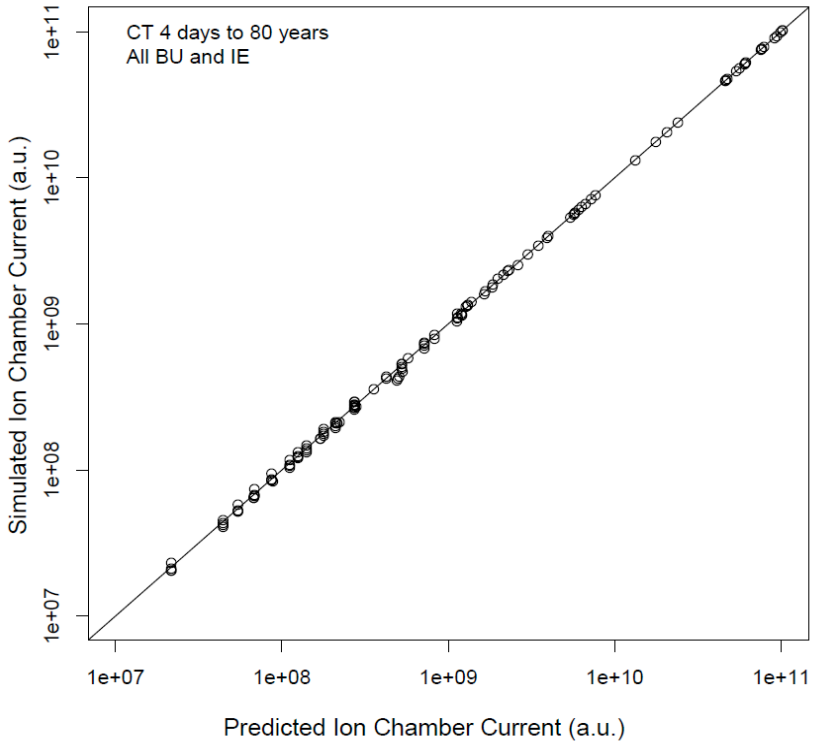

Figure 7. The simulated ion chamber current for the 8 ion chambers illustrated in Figure 1 is depicted as a function of the predicted ion chamber current for all assemblies.

Although Figures 7, indicated that Equation 2 is very successful at predicting the gamma intensity at future moments in time provided initial enrichment and burnup are known for the simulated assemblies. The results from [8] need to be emphasized which showed that assemblies with the same initial enrichment and burnup could produce very different gamma intensities, while the results from [5] indicate that the neutron count rate can be predicted later in time from just the burnup and initial enrichment.

3.2.2 Cooling time from 3.5 years to 80 years

The gamma emission from an assembly that has cooled for 3.5 years or more is dominated by ^{137}Cs, ^{154}Eu and ^{134}Cs with half-lives of 30.2, 8.60 and 2.06 years, respectively. For this reasons the following algorithm was suggested:

$$Ion\ Chamber\ Current = A + Be^{-\lambda_b t} + Ce^{-\lambda_c t} + De^{-\lambda_d t} \quad (3)$$

A, B, C and D, which are functions of initial enrichment and burnup, are constants, while λ_b, λ_c, and λ_d are the decay constants of ^{137}Cs, ^{154}Eu and ^{134}Cs, and t is time following discharge. In Figures 7, the simulated ion chamber current is graphed vs. the predicted current for 4 different initial enrichment values when each of the 28 assemblies was irradiated to 15 GWd/tU. The predictive algorithm use in Figures 8 was formed using all the 15 GWd/tU data points as input.

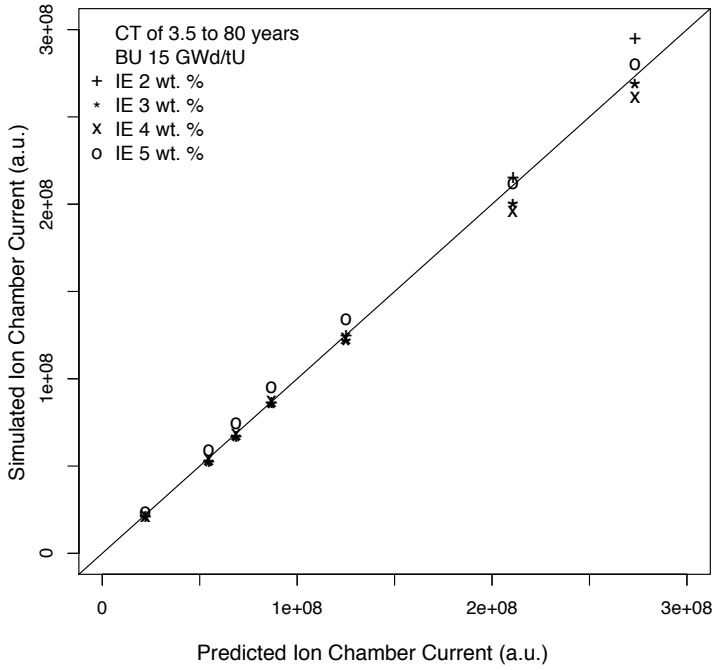

Figure 8. The simulated ion current for the 8 ion chambers illustrated in Figure 1 is depicted as a function of the predicted current for all assemblies irradiated to 15 GWd/tU for assemblies with a cooling time of 3.5 years or greater.

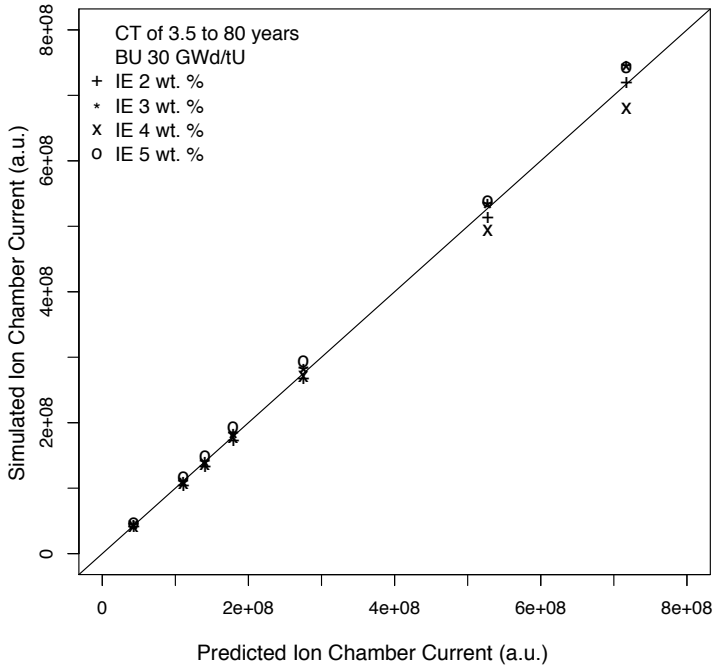

Figure 9. The simulated ion current for the 8 ion chambers illustrated in Figure 1 is depicted as a function of the predicted current for all assemblies irradiated to 30 GWd/tU for assemblies with a cooling time of 3.5 years or greater.

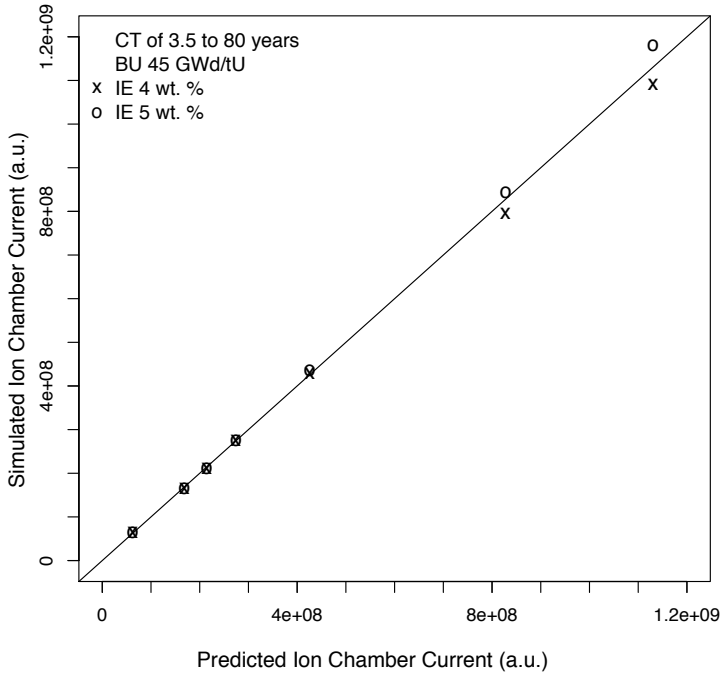

Figure 10. The simulated ion current for the 8 ion chambers illustrated in Figure 1 is depicted as a function of the predicted current for all assemblies irradiated to 45 GWd/tU for assemblies with a cooling time of 3.5 years or greater.

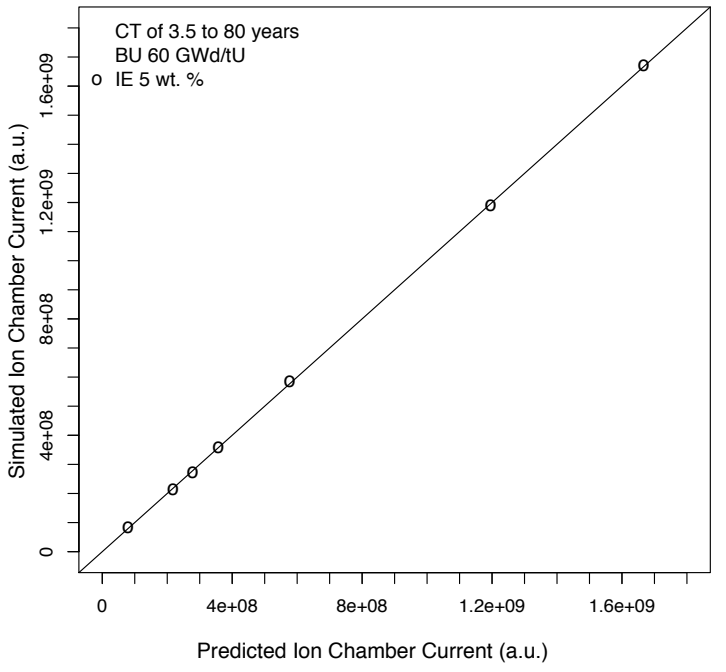

Figure 11. The simulated ion current for the 8 ion chambers illustrated in Figure 1 is depicted as a function of the predicted current for all assemblies irradiated to 60 GWd/tU for assemblies with a cooling time of 3.5 years or greater.

A conclusion from the 132 assembles simulations depicted in this section, which are illustrated in Figures 8 to 11 is that all assemblies cooled 3.5 years to 80 years can be represented accurately by the relatively simple Equation 3.

3.3 $LaBr_3$ Crystal

The resolved gamma spectra was also examined for a select number of assemblies. These assemblies, effectively considered to be "fully irradiated" assemblies, comprised of the 3 wt.% 30 GWd/tU, 4 wt.% 45 GWd/tU, and 5 wt.% 60 GWd/tU cases. The gamma spectra was examined for these assemblies at discharge (4 days) to ascertain if the 662 keV peak of ^{137}Cs could be resolved. The gamma line emitted from ^{137}Cs is commonly used burnup indicator because its production is nearly linear with burnup. The gamma spectral response simulated with a $LaBr_3$ crystal is depicted in Figures 12 to 14. A $LaBr_3$ crystal was selected because of its ability to (1) function at room temperature without cooling, (2) tolerate gamma count rates above 3 million counts per second and (3) resolve the main peaks from spent fuel with cooling times of a few years.

The FWHM at 662 keV for the $LaBr_3$ detector system is approximately 30 keV. The plots in top right corners of Figures 12 to 14 span an energy range of a little more than three FWHMs. The following observations are made from the gamma spectra of the fully depleted assembles which are illustrated in Figures 12 to 14**:**

1. The 662 keV ^{137}Cs peak is not discernable for the spectra simulated for 4 days due to the dominant 668 keV peak of ^{132}I. Note that Gaussian Energy Broadening (GEB) appropriate for a $LaBr_3$ crystal was used.

2. This 668 keV ^{132}I peak can be up to one order of magnitude stronger than the 662 keV ^{137}Cs peak at 4 days cooled, as shown in the non-GEB spectra. For the non-GEB spectra the peak widths was determined by the arbitrarily selected 3 keV-wide energy bins which was selected as part of the energy deposition tally in MCNP.

3. ^{132}I has a half-life of 2.3 hours and is mainly produced from beta decay of the fission product ^{132}Te, which has a half-life of 3.2 days. As such, during the discharge time frame of around 4 days, where the 'baseline' measurement is envisioned to be taken, a strong 662 keV ^{137}Cs peak is unattainable with a $LaBr_3$ detector due to the continual decay of ^{132}Te into ^{132}I.

4. A $LaBr_3$ spectra is expected to resolve the 662 keV ^{137}Cs peak after a cooling time of approximately one month because at that time the 668keV peak from ^{132}I will be about 1/10 the intensity of the 662 keV peak from ^{137}Cs. Note that the two peaks are only separated by 6 keV and the FWHM of the $LaBr_3$ detector is 30 keV; hence, resolving these peaks when they are similar in intensity will be challenging.

5. The preceding observations are valid for the wide range of initial enrichment and burnup cases simulated. To keep the report short, the spectral gamma plots of these other assemblies are excluded from the report.

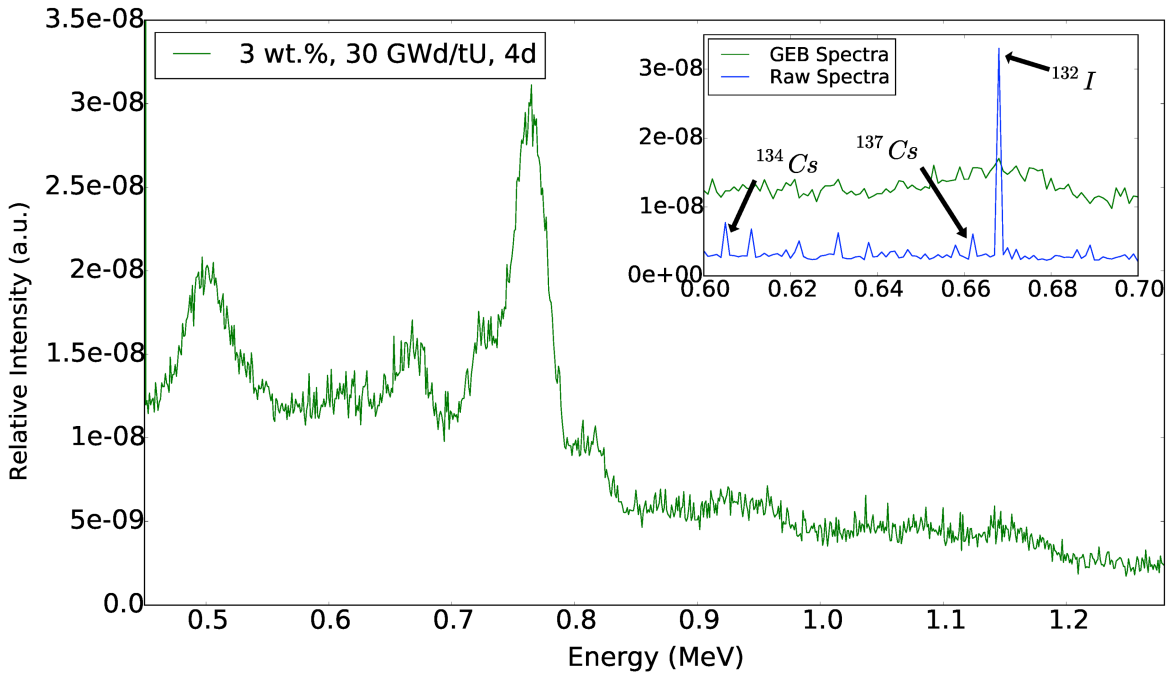

Figure 12. The Gaussian energy broadened spectral resolved gamma response from a $LaBr_3$ detector for a 3 wt.%, 30 GWd/tU assembly at discharge. The 662keV ^{137}Cs region of interest is magnified in the top right region of the plot and compared to a non-Gaussian energy broadened response.

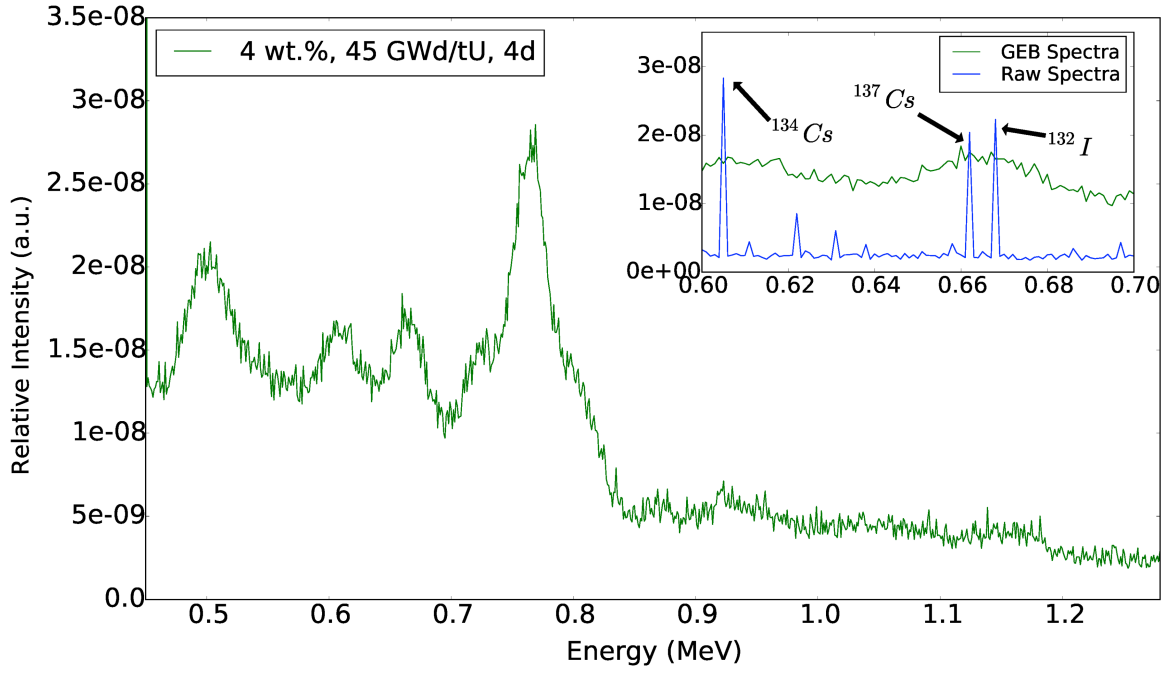

Figure 13. The Gaussian energy broadened spectral resolved gamma response from a $LaBr_3$ detector for a 4 wt.%, 45 GWd/tU assembly at discharge. The 662keV ^{137}Cs region of interest is magnified in the top right region of the plot and compared to a non-Gaussian energy broadened response.

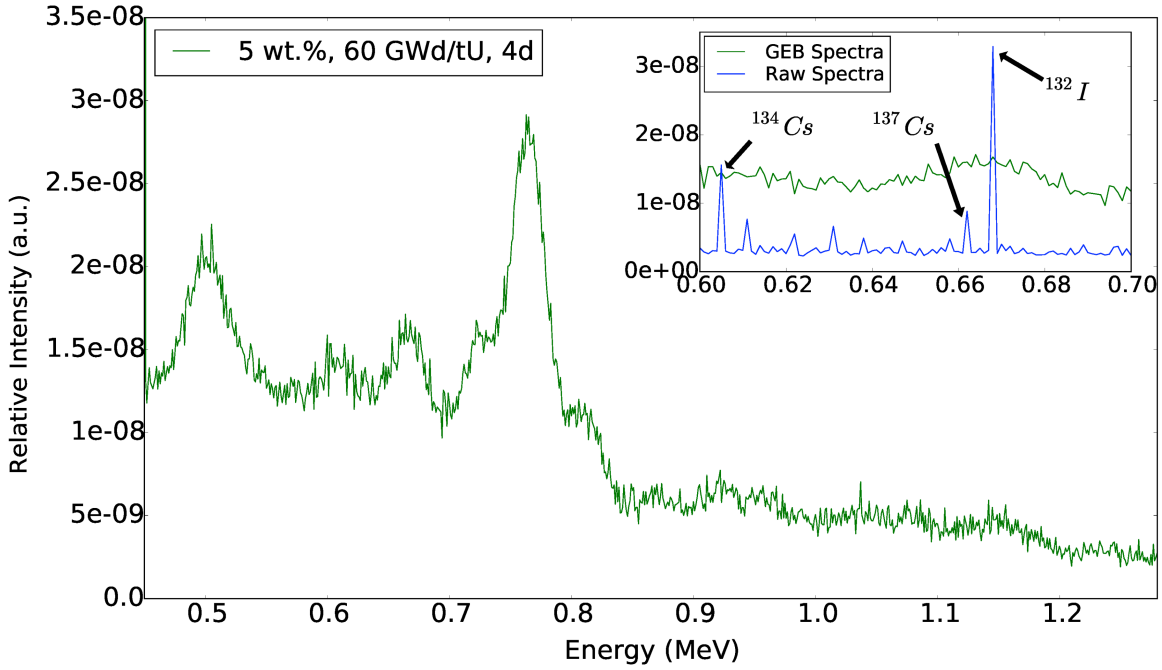

Figure 14. The Gaussian energy broadened spectral resolved gamma response from a $LaBr_3$ detector for a 5 wt.%, 60 GWd/tU assembly at discharge. The 662keV ^{137}Cs region of interest is magnified in the top right region of the plot and compared to a non-Gaussian energy broadened response.

3.4 HPGe Crystal

As in section 3.3, the resolved gamma spectra was examined for the same assemblies at discharge. These are shown in Figures 15 to 17. For these figures, the following observations are made:

1. In the GEB HPGe spectra, the 662 keV ^{137}Cs peak is discernable at discharge. This observation is similarly valid for the wide range of initial enrichment and burnup cases simulated but excluded from the report. Given that the FWHM of the simulated HPGe detector is expected to be on the order of 2 keV, resolution of peaks separated by 8 keV is expected.

2. One undesirable property of a HPGe detector for the deployment of interest here is the need to provide active cooling to the detector. This is not a concept-ending characteristic given the standard use of mechanical coolers with HPGe detectors.

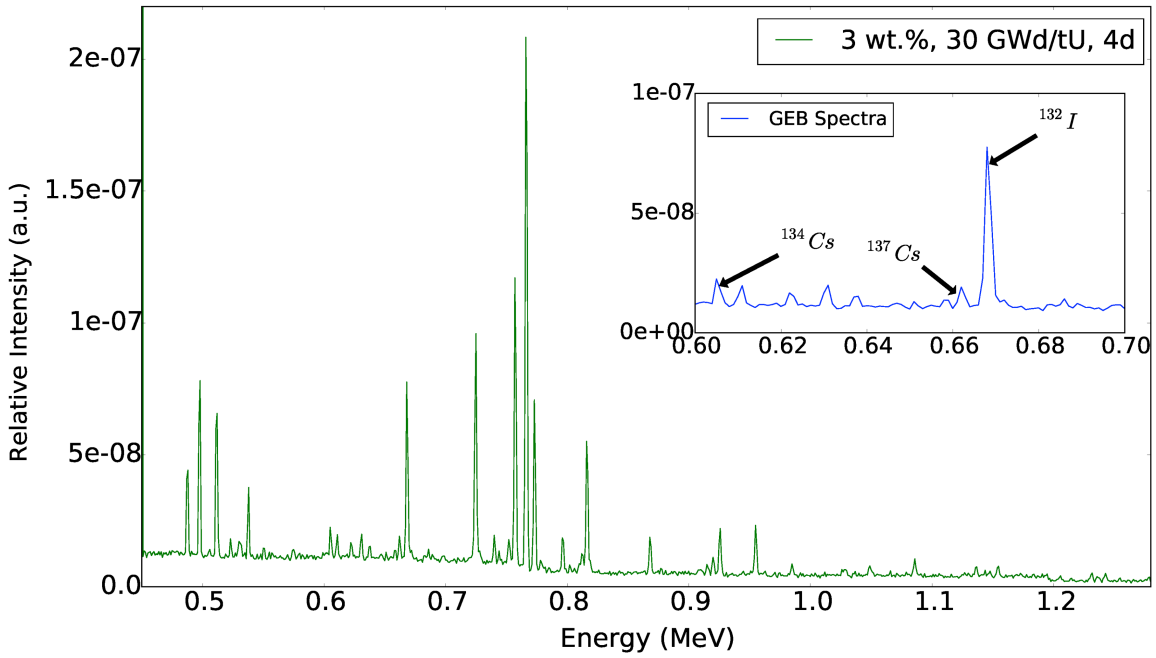

Figure 15. The Gaussian energy broadened spectral resolved gamma response from a HPGe detector for a 3 wt.%, 30 GWd/tU assembly at discharge. The Gaussian energy broadened 662keV ^{137}Cs region of interest is magnified in the top right region of the plot.

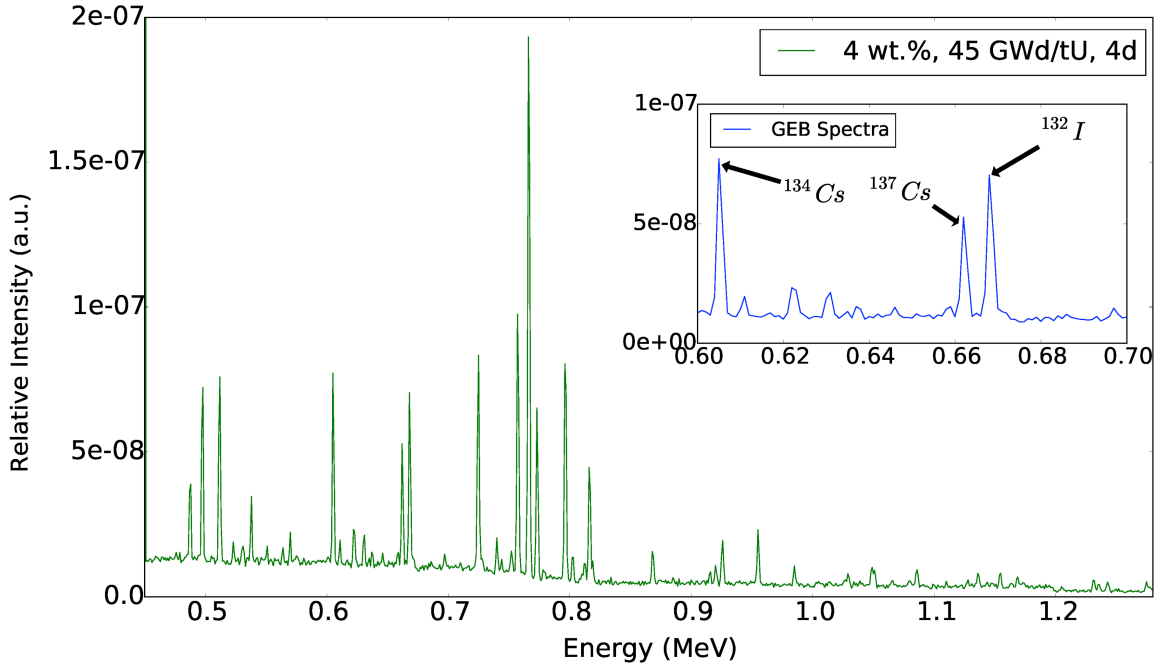

Figure 16. The Gaussian energy broadened spectral resolved gamma response from a HPGe detector for a 4 wt.%, 45 GWd/tU assembly at discharge. The Gaussian energy broadened 662keV ^{137}Cs region of interest is magnified in the top right region of the plot.

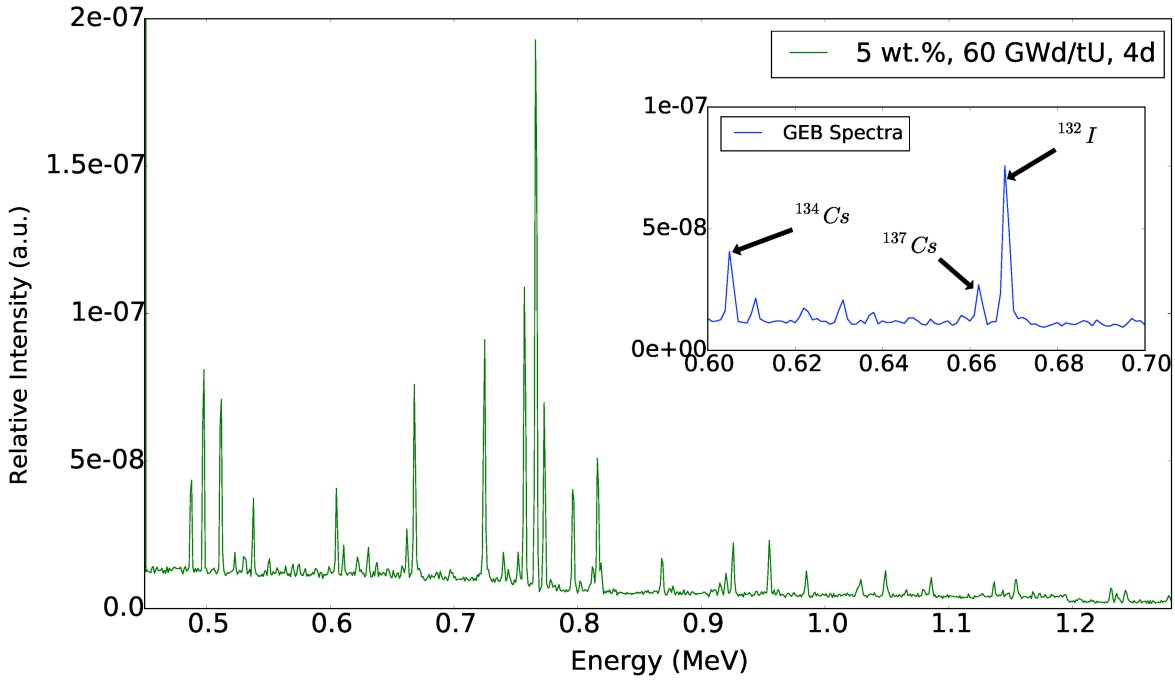

Figure 17. The Gaussian energy broadened spectral resolved gamma response from a HPGe detector for a 5 wt.%, 60 GWd/tU assembly at discharge. The Gaussian energy broadened 662keV ^{137}Cs region of interest is magnified in the top right region of the plot.

4 Discussion of Simulated Signals in Context of Two Technical Goals

Below each of the two technical goals are discussed in separate subsections for the purpose describing what was learned throughout FY16 as well as to outline recommended future research.

4.1 Can safeguards benefit from modern irradiation practices?

In the context of assessing if modern irradiation practices can help safeguards, we plan to use information about assemblies irradiated throughout the decades of commercial nuclear power plant operation. During this initial phase of this research, we obtained a database from the U.S. Energy Information Administration containing assembly characteristics of over 244,000 assemblies irradiated in the USA from 1962 until 2013.

The database only describes the fuel and not the simulated gamma and neutron signatures. Yet, we can leverage our simulated neutron results because we know that if the initial enrichment and burnup of that assembly is known, we can accurately predict the neutron count rate into the future. Hence, if the database shows that the burnup for a given initial enrichment varies less in modern fuel as compared to older fuel, we can conclude that the neutron count rate will also vary less. Furthermore, since we can predict the neutron intensities well, our predicted signals will vary less for modern fuel as compared for older fuel.

Below we outline our suggested future research path to advance this line of research.

1. Select assemblies of the **same/similar fuel type(s)** irradiated between 1965 and 1975.
    a. Subdivide the selected database into subgroups based on a **narrow initial enrichment ranges**. The range selection is to be guided by the need to have enough assemblies in the selected group to have good statistics. Initial exploration of the

database indicates that the inclusion of approximately 1000 assemblies in an initial enrichment grouping is reasonable. It would be interesting to select several narrow initial enrichment ranges between 2.8 and 5.0 GWd/tU.

b. For each initial enrichment subgroup, **quantify the standard deviation in the burnup** range of these assemblies. By comparing the one sigma percentage variation in fuel created early in the commercial fuel to that which was created more recently, we can gain insight into how much the total neutron and passive gamma intensities would vary between old and modern fuel.
    i. An important follow up question is if the quoted burnup values represent the values calculated at the time of irradiation or if they were updated to reflect modern code/data capability.

2. Repeat the same process outlined in step 1 above except for different decades. The interval between 2002 and 2012 is the most modern decade. It would be convenient to select two more decade intervals between the two already suggested intervals (1965 to 1975 and 2002 to 2012). If the process was automated and the statistics are good it may be possible to reduce the time interval from a decade to grouping of 5 years.

4.2 Is there merit to measuring spent fuel attributes from cradle-to-grave?

Compared to the status quo of spent fuel monitoring; which involves (1) looking at the **qualitative** glow of the water around the assembly, and/or (2) measuring, in **temporal isolation**, the total neutron and passive gamma intensity from a **subset** of assemblies, **measuring all assemblies at discharge and every time the fuel is moved subsequently with an automated system that compares among measurements is expected to improve safeguards significantly**.

The value of measuring at discharge: By measuring the total neutron count rate and the gross gamma intensity at discharge, approximately at 4 days cooled, a few pieces of data are tied together: the moment in time when the measurement was made is connected to the measured intensities. **This connection does not exist today.** The work presented in this report indicates that the decrease in the measured neutron count rate can be accurately predicted in the future if the initial enrichment and burnup of the assembly are known. Using this declared data, as known values may be acceptable. Another option, which needs further research, is to see if the need for declared data could be relaxed. Such a relaxation would need to leverage either additional measurements signatures from the fuel or systematic factor about the fuel such as being able to "treat all assemblies as if they are fully irradiated."

From the results in this paper we conclude that if we measure an assembly at discharge and we know the initial enrichment and burnup of that assembly, we can accurately predict the neutron count rate into the future. Hence, if a significant number of pins were taken, the neutron count rate along could indicate this within the uncertainty limit of our prediction.

The value of including passive gamma measurements: The initial hope was that the ion chamber results would provide a complimentary tool to the neutron measurement because it is such a simple robust detector. However, as described in [8], the total passive gamma measurement made at discharge can have difficult to predict dependencies. This discovery is a very valuable lesson learned but not encouraging for using ion chamber data with the cradle-to-grave monitoring concept. The next step was then to see if spectral resolved gamma data would help as it provides the ability to focus in on the evolution of specific isotopes, rather than all isotopes summed together as is the case with an ion chamber. A $LaBr_3$ detector was initially selected given several positive properties of

this detector material specific to the spent fuel measurement context already discussed in this paper. Yet, the key lesson learned was that $LaBr_3$ detector was not able to resolve the one gamma peak that is known to have a well predicted behaviour between discharge to disposal, the 662 keV peak of ^{137}Cs. We went a step further to see if this key peak could be resolved by a HPGe detector and learned that it could. Unfortunately this detector needs active cooling, which complicates deployment. Yet, the concept works with HPGe. Future research could explore how much including of the 662 keV peak in all spectra might help.

5 Conclusions

Through this research effort the following conclusions were reached:

1. The total neutron count rate can be accurately predicted at any future moment in time based upon the measured count rate at discharge, provided the initial enrichment and burnup of the assembly is known at discharge. Experimental data needs to accurately quantify the uncertainties on this claim but the simulation results are promising.

2. Given that the vast majority of assemblies are fully irradiated, meaning that the initial enrichment and burnup are tightly coupled, it is expected that the total neutron count rate measured at discharge will be indicative of the initial enrichment and burnup of that assembly. Yet, the fact that all assemblies are not fully irradiated means an additional approach is needed to manage these non-fully irradiated assemblies is needed.

3. The theses that more useful safeguards conclusions can be made for modern assemblies as compared to older assemblies when these assemblies are measured with an instrument such as a Fork detector was not fully answered but it was advanced. A research path was outlined. The data necessary to advance that research path was obtained. The next step is to implement that path.

One final conclusion is listed below. It is listed separately from the other conclusions because it represents an evolution in the thinking of the researchers on a high level. We think that, in the course of doing this research, we have developed a more useful approach. Here are some of our thought which have contributed to this evolution:

1. A weak point in the approach described in this report is that the assembly can only be measured when it is out of the rack or reactor. In general **all assemblies are only available at two moments in their lives**: (1) at discharge and (2) just before entering either dry storage or a repository-ready container. Hence, the inspectorate is only sure of two measurements. It is possible to request an assembly during an inspection but practically speaking only a few assemblies can be measured during an inspection. If the predictive algorithms using only data from discharge are very predictive, it could still be of considerable use if COK were lost.

2. **If the automated robot were to focus on measuring the assemblies in the rack without moving them the time available would increase immensely**. The practical reality is that implementation of the cradle-to-grave concept as proposed in this research effort allows for only around 5 minutes to make a measurement. This is the limit because that is how long it takes a crane operator to insert an assembly in the rack. If the robot focused on the assemblies in the rack then they have nearly every minute of the year to measure the assembly. Furthermore the robot could become large, have shielding for detector and move slowly and measure for long periods of time. NDA options could increase to include multispectral options (IR, UV, visible, gamma, sonic, etc.). The hardware could overcome some of the negative attributes of a current DCVD deployment. Repeat measurements

would be easy and it might be possible to look around obstacles on the top of an assembly as the instrument are ~0.5 meters from the fuel rather than 154 meters above the fuel in current DCVD deployments.

3. The cradle-to-grave approach advocated in this paper needs to have a measurements at discharge. Hence, it is not able to help with much of the ~60 years worth of fuel already in pools. **However, a robot moving in the space above the fuel rack, repeatedly measuring all the assemblies currently in the rack, can establish reference measurements for all assemblies in existence.**

6 References

[1] J. D. Galloway et al., "Design and Description of the NGSI Spent Fuel Library with an Emphasis on Passive Gamma Signal," Journal of Nuclear Materials Management, 40(3), 25-35 (2012).

[2] H. R. Trellue, J.D. Galloway, N.A. Fischer, and S.J. Tobin, "Advances in Spent Fuel Libraries," Proceedings of Institute of Nuclear Materials Management 54th Annual Meeting, Palm Desert, California (2013).

[3] D. Reilly, N. Ensslin, H. Smith, Jr., editors, "Passive Nondestructive Assay of nuclear Materials," Los Alamos National Laboratory Report, LA-UR-90-732, (1990).

[4] J. K. Tuli, "Nuclear Wallet Cards," National Nuclear Data Center, Brookhaven National Laboratory, (2011).

[5] B. J. Adigun, S. J. Tobin, H. R. Trellue, M. L. Fensin, M. L. Fugate, G. J. Dean, J. R. Tutt, and J. K. Sprinkle, "Enabling Comparative Neutron Measurements of Spent Fuel Assemblies for Nonproliferation Purposes," Los Alamos National Laboratory Report, LA-UR-16-22178, (2016).

[6] J. Hu, I.C. Gauld, J. Banfield and S. Skutnik, "Developing Spent Fuel Assembly Standards for Advanced NDA Instrument Calibration - NGSI Spent Fuel Project," Oak Ridge National Laboratory Report, ORNL/TM-2013/576, February 2014.

[7] S. J. Tobin et al., "Determining Plutonium in Spent Fuel with Nondestructive Assay Techniques," Los Alamos National Laboratory Report, LA-UR-09-03180, (2009).

[8] B. J. Adigun, H. R. Trellue, G. J. Dean, S. J. Tobin, and J. D. Galloway, "The Effect of Localized Pin Flux on Short-Term Gamma Intensities of Spent Fuel Assemblies," Los Alamos National Laboratory Report, LA-UR-16-2448, (2016).